Available online at www.sciencedirect.com

SCIENCE DIRECT®

Lithos 83 (2005) 255–276

LITHOS

www.elsevier.com/locate/lithos

Geochemistry of cumulates from the Bjerkreim–Sokndal layered intrusion (S. Norway) Part II. REE and the trapped liquid fraction

Bernard Charlier*, Jacqueline Vander Auwera, Jean-Clair Duchesne

Department of Geology, Bldg B20, University of Liège, B 4000 Sart Tilman, Belgium

Received 1 November 2003; accepted 18 February 2005
Available online 25 April 2005

Abstract

Rare earth elements in bulk cumulates and in separated minerals (plagioclase, apatite, Ca-poor and Ca-rich pyroxenes, ilmenite and magnetite) from the Bjerkreim–Sokndal layered intrusion (Rogaland Anorthosite Province, SW Norway) are investigated to better define the proportion of trapped liquid and its influence on bulk cumulate composition. In leuconoritic rocks (made up of plagioclase, Ca-poor pyroxene, ilmenite, ±magnetite, ±olivine), where apatite is an intercumulus phase, even a small fraction of trapped liquid significantly affects the REE pattern of the bulk cumulate, together with cumulus minerals proportion and composition. Contrastingly, in gabbronoritic cumulates characterized by the presence of cumulus Ca-rich pyroxene and apatite, cumulus apatite buffers the REE content. La/Sm and Eu/Eu* vs. P_2O_5 variations in leuconorites display mixing trends between a pure adcumulate and the composition of the trapped liquid, assumed to be similar to the parental magma. Assessment of the trapped liquid fraction in leuconorites ranges from 2 to 25% and is systematically higher in the north-eastern part of the intrusion. The likely reason for this wide range of TLF is different cooling rates in different parts of the intrusion depending on the distance to the gneissic margins. The REE patterns of liquids in equilibrium with primitive cumulates are calculated with mass balance equations. Major elements modelling (Duchesne, J.C., Charlier, B., 2005. Geochemistry of cumulates from the Bjerkreim–Sokndal layered intrusion (S. Norway): Part I. Constraints from major elements on the mechanism of cumulate formation and on the jotunite liquid line of descent. Lithos. 83, 299–254) permits calculation of the REE content of melt in equilibrium with gabbronorites. Partition coefficients for REE between cumulus minerals and a jotunitic liquid are then calculated. Calculated liquids from the most primitive cumulates are similar to a primitive jotunite representing the parental magma of the intrusion, taking into account the trapped liquid fraction calculated from the P_2O_5 content. Consistent results demonstrate the reliability of liquid compositions calculated from bulk cumulates and confirm the hypothesis that the trapped liquid has crystallized as a closed-system without subsequent mobility of REE in a migrating interstitial liquid.

Keywords: Bjerkreim–Sokndal; Layered intrusions; Cumulates; Rare Earth elements; Trapped liquid; Jotunite

* Corresponding author. Tel.: +32 4 3662250; fax: +32 4 3662921.
E-mail address: b.charlier@ulg.ac.be (B. Charlier).

0024-4937/$ - see front matter © 2005 Elsevier B.V. All rights reserved.
doi:10.1016/j.lithos.2005.03.005

1. Introduction

Reconstructing the missing link between cumulates and liquids, i.e., the composition of cumulates related to series of liquids obtained from quenched rocks or, inversely, the composition of liquids in equilibrium with exposed cumulates, is a major challenge in igneous petrology. A data set of partition coefficients is classically used to assess the trace element content of liquids by an inversion calculation. The problem in estimating liquid compositions from cumulus minerals is that, in a slow cooling magma chamber, postcumulus processes (e.g., Sparks et al., 1985) such as fluid transfer (Irvine, 1980; Meurer et al., 1997), trapped liquid crystallization (see Barnes, 1986 for major elements and Cawthorn, 1996 for incompatible trace elements), or in general subsolidus redistribution of elements between minerals, can modify the original high-temperature magmatic composition. Because of the late-enrichment of incompatible elements by percolating fluids or trapped liquid, the inversion calculation often results in overestimation of the incompatible element content of the magma. In order to avoid this problem, Cawthorn et al. (1991), Cawthorn (1996) and Bédard (1994, 2001) have proposed models which are not simple inversion calculations, but are based on a mass balance equation which takes into account the trapped liquid fraction (TLF). This modelling is based on whole-rock compositions, modal proportions of cumulus minerals and partition coefficients. Moreover, it relies on the assumption that the trapped liquid has crystallized as a closed-system.

In a companion paper (Duchesne and Charlier, 2005), whole-rock major element compositions of cumulates from the Bjerkreim–Sokndal layered intrusion (BKSK), situated in the Proterozoic Rogaland Anorthosite Province (SW Norway), were discussed in order to bring new constraints on crystallization processes of cumulates. We have calculated cotectic assemblages and defined differentiation process, including the liquid line of descent. Here we investigate the REE composition of bulk cumulates and of some mineral separates. These incompatible elements are largely influenced by the amount of interstitial liquid and thus are particularly well suited to trace the trapped liquid shift on bulk rocks and on cumulus minerals compositions.

Mass balance calculations are applied to cumulates from BKSK. Calculated REE contents of liquids in equilibrium with these cumulates are compared with primitive liquids represented by fine-grained jotunites (chilled margins) which are interpreted to be the parental magma of BKSK (Duchesne and Hertogen, 1988; Vander Auwera and Longhi, 1994; Robins et al., 1997). Prior to this modelling, the REE content of cumulates is discussed to establish the factors controlling the concentration of these elements and whether, as postulated by Maier and Barnes (1998), it is mainly governed by the trapped liquid composition.

Our results indicate that both cumulus minerals and trapped liquid play an important role in governing the REE distribution of bulk cumulates. They also enable us to constrain the TLF in the BKSK cumulates, previously described as adcumulates (Duchesne, 1978), and to demonstrate the reliability of liquid compositions calculated from cumulates with a consistent partition coefficients dataset. They finally confirm the assumption that the trapped liquid has crystallized as a closed-system.

2. BKSK and associated liquids

BKSK (Michot, 1960; Duchesne, 1987; Wilson et al., 1996; Duchesne, 2001) exposes the "Layered Series" in the Bjerkreim lobe (Fig. 1), which consists of a 7000 m-thick sequence of cumulates made up of anorthosite, troctolite, leuconorite, norite, gabbronorite, jotunite and mangerite. The massive upper part of the intrusion comprises quartz mangerites and charnockites, mostly representing liquid compositions (Duchesne and Wilmart, 1997). The Layered Series is subdivided into five megacyclic units (MCU IA, IB, II, III and IV). The base of each MCU usually displays a compositional reversal to more primitive mineral compositions as a result of new magma influxes (Duchesne, 1972; Nielsen and Wilson, 1991; Jensen et al., 1993; Wilson et al., 1996; Barling et al., 2000; Jensen et al., 2003). The MCUs are subdivided into zones (a to f), based on the cumulus mineral assemblages (Wilson et al., 1996). Plagioclase is the first cumulus mineral to appear and is present throughout the entire sequence. It is followed by ilmenite, slightly before Ca-poor pyroxene. Magnetite precedes apatite and Ca-rich pyroxene, which appear

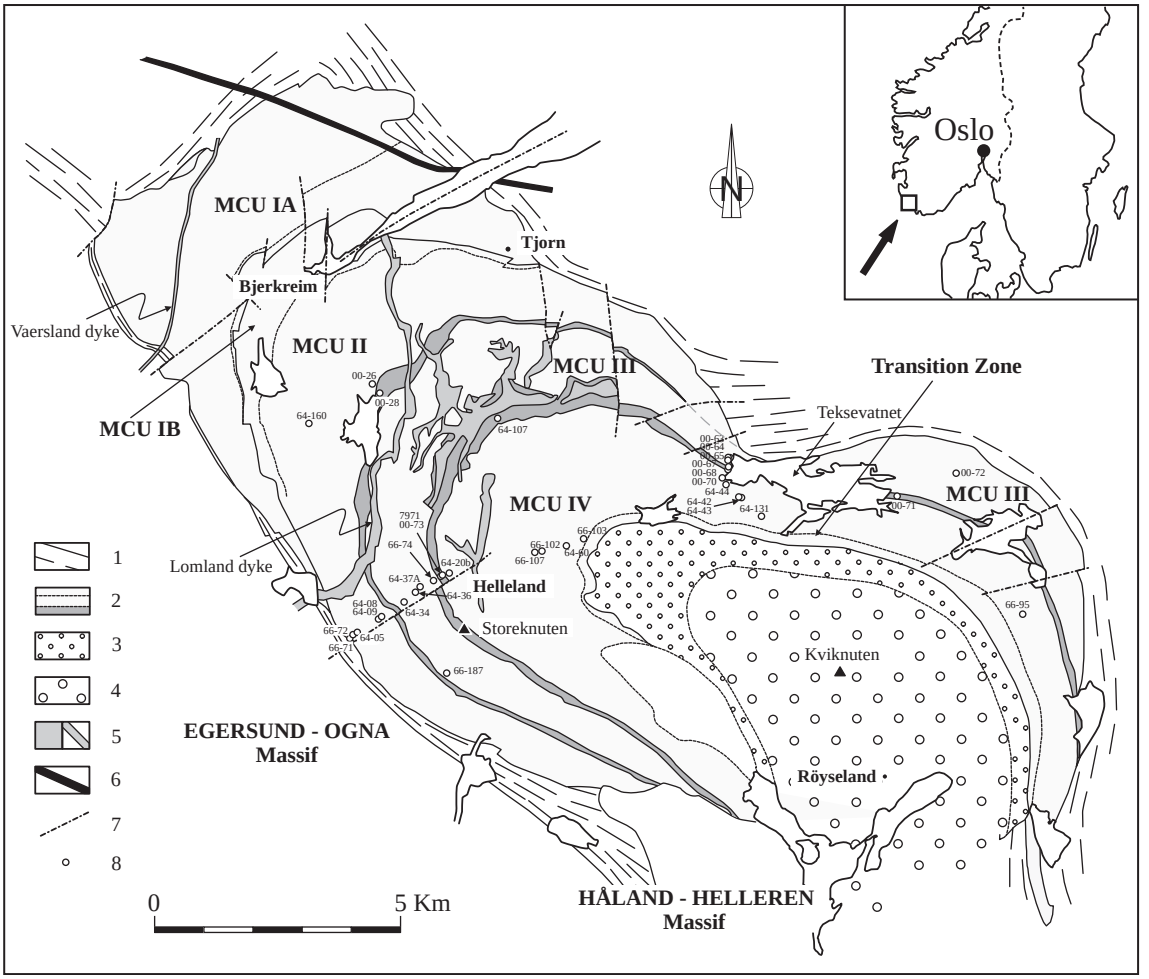

Fig. 1. Geological map of the Bjerkreim lobe of the Bjerkreim–Sokndal layered intrusion, showing sample locations and boundaries for megacyclic units (MCU). (1) Granulitic gneisses; (2) the Layered Series with troctolite (pimo-C) at the base of MCU III and IV; (3) mangerite; (4) quartz mangerite and charnockite; (5) Lomland and Vaersland dykes; (6) Doleritic dyke; (7) Fault; (8) samples location.

simultaneously. At the top of MCU IV, hypersthene is replaced by inverted pigeonite. At the base of MCUs III and IV (zone b), the magma crystallizes temporally olivine and magnetite instead of hypersthene. Variations of silica activity and oxygen fugacity would have increased the stability of olivine relative to hypersthene (Wilson et al., 1996). Cumulus plagioclase crystals display strong recrystallization to polygonal grains. Pyroxenes are usually kinked and oxides have acquired interstitial habits. This thermal annealing, which gave rise to severe grain-shape modifications, is associated with a late foliation and lineation which has overprinted the primary orientation of cumulus grains. These deformations resulted from a gravity-controlled subsidence of the magma chamber floor due to the high density contrast with the host anorthosite and broadly granitic gneisses under high thermal conditions (Paludan et al., 1994; Bolle et al., 2000, 2002). Recrystallization has, in many places, completely overprinted the original cumulate texture. Mineral zoning is absent but plagioclase displays compositional variations between individual grains, possibly due to recrystallization of initially zoned minerals (Wilson et al., 1996). The petrography does not permit any evaluation of the residual porosity as done by Morse (1979) for

Table 1
REE and selected major element contents of the jotunitic parental magma and of bulk cumulates from megacyclic units II, III and IV of BKSK

Sample No.	80.12.3a[a]	66-71	66-72	64-05	64-160	00-72	64-08	64-09	00-26	00-28	66-187	00-63
MCU	Jotunite	II	II	II	II	II	II	II	II	III	III	III
		pih-C	pih-C	pih-C	pih-C	pih-C	pih-C	pih-C	pih-C	pimo-C	pih-C	pih-C
SiO_2 (%)[b]	49.39	51.42	50.77	48.06	52.12	49.92	45.77	47.49	53.61	50.00	43.45	45.83
Al_2O_3	15.81	22.99	20.65	18.31	24.54	20.38	17.23	17.67	19.35	23.82	13.40	16.23
TiO_2	3.67	2.84	3.14	4.45	2.45	3.54	5.41	4.68	3.49	2.12	7.38	6.45
MgO	4.54	2.84	4.97	6.69	1.34	5.22	7.61	7.36	3.41	3.35	11.04	7.68
P_2O_5	0.71	0.04	0.01	0.10	0.11	0.12	0.05	0.04	0.07	0.04	0.01	0.16
La (ppm)	23.90	3.66	2.96	2.66	2.73	4.72	1.98	1.71	2.18	2.94	1.90	4.68
Ce	58.00	8.01	5.89	5.32	5.74	10.00	3.89	3.67	4.03	5.14	3.87	11.02
Pr	–	0.89	0.58	0.53	0.64	1.19	0.32	0.35	0.50	0.56	0.44	1.34
Nd	39.00	3.62	2.09	2.10	2.19	5.58	1.41	1.35	1.94	2.32	1.47	6.17
Sm	8.50	0.65	0.42	0.46	0.49	1.05	0.31	0.31	0.33	0.27	0.40	1.31
Eu	2.86	1.13	0.94	0.81	0.95	1.07	0.65	0.64	0.78	0.92	0.54	0.97
Gd	–	0.57	0.36	0.40	0.45	0.97	0.37	0.35	0.31	0.26	0.45	1.24
Tb	1.13	0.07	0.05	0.07	0.07	0.14	0.03	0.04	0.05	0.04	0.08	0.19
Dy	–	0.46	0.33	0.42	0.30	0.76	0.37	0.34	0.30	0.16	0.51	0.97
Ho	–	0.08	0.08	0.11	0.07	0.17	0.08	0.08	0.08	0.04	0.11	0.20
Er	–	0.19	0.18	0.22	0.14	0.38	0.22	0.18	0.21	0.08	0.35	0.47
Tm	–	0.03	0.03	0.03	0.01	0.05	0.03	0.03	0.03	0.01	0.06	0.07
Yb	2.00	0.18	0.18	0.22	0.10	0.33	0.21	0.17	0.22	0.08	0.37	0.42
Lu	0.33	0.02	0.02	0.03	0.01	0.05	0.03	0.03	0.03	0.01	0.06	0.06
Y	22.00	2.20	1.18	1.05	0.81	4.10	0.72	0.67	2.10	0.94	2.89	5.00
Total REE	135.72	19.56	14.11	13.38	13.89	26.46	9.90	9.25	10.99	12.83	10.61	29.11
La/Sm	2.81	5.63	7.05	5.78	5.57	4.50	6.39	5.52	6.61	10.89	4.75	3.57
Eu/Eu*	1.06	5.68	7.39	5.77	6.19	3.24	5.87	5.94	7.46	10.62	3.89	2.33
$(La/Yb)_N$	8.57	14.59	11.80	8.67	19.58	10.26	6.76	7.22	7.11	26.36	3.68	7.99

[a] Data from Duchesne and Hertogen (1988).
[b] Major elements from Duchesne and Charlier (2005).

Kiglapait because, as underlined by Hunter (1996), a recrystallized orthocumulate could develop the texture of an adcumulate. Assessment of the trapped liquid abundance must therefore be investigated chemically rather than petrographically.

BKSK and, in general, the Rogaland Anorthosite Province, is associated with typical liquids of the AMC (Anorthosite–Mangerite–Charnockite) series. The least evolved melts are jotunite (Fe–Ti–P-rich hypersthene monzodiorite). These liquids, called "primitive jotunites" by Vander Auwera et al. (1998b), occur as chilled margins to intrusions such as Hidra (Duchesne and Demaiffe, 1978; Demaiffe and Hertogen, 1981) and BKSK (Duchesne and Hertogen, 1988; Vander Auwera and Longhi, 1994; Robins et al., 1997). They are considered to represent parental magmas to these large intrusions and also to andesine anorthosites (Duchesne et al., 1974; Vander Auwera et al., 1998b). Fractional crystallization of primitive jotunite magma drives the melt to more evolved liquid compositions, successively evolved jotunite, mangerite, quartz mangerite and charnockite. The Tellnes dyke (Wilmart et al., 1989) exposed a continuous evolution from evolved jotunite to charnockite, accounted for by closed-system fractional crystallization. The liquid line of descent of the jotunite suite has been presented by Vander Auwera et al. (1998b). REE variations of these rocks have been extensively documented and discussed by Duchesne and Demaiffe (1978), Duchesne et al. (1985), Duchesne et al. (1989), Wilmart et al. (1989), Vander Auwera et al. (1998b) and Bolle et al. (2003). Globally, the REE content significantly increases from primitive to evolved jotunite and then, after the appearance of liquidus apatite, remains more or less constant towards mangerites and quartz

00-64	64-34	64-36	64-37A	64-107	00-67	00-71	00-73	7971	64-20b	00-68	00-65
III	III	III	III	IV	IV	IV	IV	IV	IV	IV	III
pihm-C	pihm-C	pihm-C	pihm-C	pih-C	pimo-C	pimo-C	pimo-C	pimo-C	pih-C	pih-C	pihmac-C
46.77	45.74	48.27	47.41	51.33	48.03	47.45	50.14	49.66	52.77	55.39	45.90
17.84	15.51	18.72	17.50	20.01	21.02	20.48	23.05	20.77	19.70	24.44	16.93
4.72	5.51	3.86	3.82	2.91	3.60	3.81	2.48	2.82	2.12	0.88	3.06
6.11	8.24	5.41	5.75	6.05	4.88	5.14	3.76	4.42	4.06	1.53	4.97
0.10	0.02	0.04	0.12	0.04	0.19	0.17	0.05	0.05	0.02	0.09	3.49
3.91	1.89	4.30	2.12	1.65	6.50	5.48	2.88	2.31	1.64	3.68	21.64
8.30	3.98	6.70	4.25	3.37	12.38	12.17	5.24	5.20	3.84	7.36	57.79
1.00	0.46	0.59	0.45	0.40	1.54	1.50	0.57	0.47	0.37	0.83	8.42
4.36	2.00	1.93	1.52	1.66	6.95	7.04	2.22	1.78	1.07	3.55	43.04
0.98	0.42	0.45	0.36	0.27	1.48	1.42	0.31	0.36	0.22	0.59	10.72
0.99	0.66	0.86	0.36	0.77	1.18	1.16	0.90	0.91	0.92	1.25	3.16
0.89	0.39	0.50	0.35	0.23	1.34	1.31	0.23	0.35	0.29	0.53	9.46
0.13	0.06	0.06	0.06	0.04	0.17	0.17	0.03	0.05	0.04	0.07	1.14
0.68	0.41	0.37	0.34	0.18	0.88	0.88	0.14	0.23	0.23	0.35	5.47
0.14	0.09	0.08	0.07	0.05	0.18	0.18	0.03	0.05	0.05	0.07	1.08
0.32	0.24	0.18	0.19	0.10	0.41	0.38	0.07	0.10	0.12	0.15	2.04
0.05	0.04	0.03	0.03	0.02	0.06	0.05	0.01	0.01	0.02	0.02	0.24
0.30	0.23	0.16	0.19	0.08	0.29	0.31	0.06	0.08	0.11	0.12	1.21
0.05	0.03	0.02	0.03	0.01	0.03	0.04	0.01	0.01	0.02	0.02	0.14
3.30	1.07	0.87	0.86	1.54	4.60	4.90	0.85	0.38	0.19	1.80	25.00
22.10	10.90	16.23	10.32	8.83	33.39	32.09	12.70	11.91	8.94	18.59	165.55
3.99	4.50	9.56	5.89	6.11	4.39	3.86	9.29	6.42	7.45	6.24	2.02
3.24	4.99	5.54	3.10	9.45	2.56	2.60	10.30	7.84	11.14	6.83	0.96
9.35	5.89	19.28	8.00	14.79	16.08	12.68	34.43	20.71	10.69	22.00	12.83

(continued on next page)

mangerites. Jotunite, evolved jotunite, mangerite and quartz mangerite are always LREE-enriched (average $(La/Yb)_N$=~9). Eu anomalies are not significant and are either slightly negative or positive.

3. Sampling and presentation of data

Samples have been collected from the Layered Series of the Bjerkreim lobe (Fig. 1). Variations of major elements for cumulates of MCU II to IV have been presented by Duchesne and Charlier (2005). Among the samples used in that study, 34 samples have been selected for REE analyses by ICP-MS (Table 1). Some cumulus minerals (9 plagioclases, 11 apatites, 2 Ca-poor and 2 Ca-rich pyroxenes, 1 ilmenite and 1 magnetite) have been separated using dense liquids and a Frantz isodynamic magnetic separator. Prior to analyses, plagioclases, pyroxenes and oxides were leached with HCl in order to dissolve any apatite from composite grain or as inclusions. The REE content of separated minerals has been determined by ICP-MS following the method of Vander Auwera et al. (1998a) (Table 2). The analyses were carried out at the Collectif Interinstitutionnel de Géochimie Instrumentale, Université de Liège (ICP-MS is a VG Plasma Quad PQ2 of Fisons Instruments). Six apatite analyses of Roelandts and Duchesne (1979) are also integrated with the new apatite analyses. Some plagioclases previously analysed by Roelandts and Duchesne (1979) by NAA at the Mineralogisk–Geologisk Museum (Oslo University) have been reanalysed by ICP-MS. The agreement between the two methods is excellent for LREE but we find now much higher values for the HREE.

Table 1 (*continued*)

Sample No.	66-74	64-44	64-42	64-43	00-70	66-95	66-107	64-131	66-102	64-60	66-103
MCU	III	IV	IV	IV	IV	IV	IV	IV	IV	IV	IV
	pihmac-C	pihmac-C	pihmac-C	pihmac-C	pihmac-C	pihmac-C	pih'mac-C	pih'mac-C	pih'mac-C	pih'mac-C	pih'mac-C
SiO_2 (%)[b]	42.58	35.46	48.73	41.92	40.42	38.77	45.00	47.62	43.55	44.61	42.11
Al_2O_3	14.78	6.05	19.22	11.70	9.40	11.63	14.80	15.85	13.02	13.43	11.67
TiO_2	3.76	6.55	2.29	4.33	5.15	5.82	3.30	2.80	3.80	3.37	4.05
MgO	5.52	11.43	3.16	7.56	10.20	6.88	5.44	3.86	5.95	5.46	6.25
P_2O_5	3.23	4.52	1.87	3.33	3.96	3.82	2.36	1.88	2.78	2.44	3.02
La (ppm)	15.00	27.31	16.40	23.06	24.78	28.60	22.60	28.90	26.56	26.10	32.90
Ce	41.70	74.70	43.22	64.51	66.21	75.52	55.40	72.68	70.48	66.59	85.60
Pr	6.82	12.40	5.93	10.25	10.35	11.97	8.64	10.72	10.91	10.27	13.49
Nd	33.85	62.85	32.24	50.36	54.26	59.64	40.40	51.75	54.41	50.05	67.70
Sm	8.94	15.00	7.60	12.65	13.14	14.42	9.62	12.27	13.27	11.90	15.57
Eu	2.84	3.69	2.68	3.50	3.42	4.01	2.96	4.79	4.60	4.52	5.37
Gd	8.16	13.56	6.82	10.69	12.56	13.68	8.12	11.11	12.14	10.56	14.62
Tb	1.13	1.86	0.94	1.53	1.56	1.73	1.08	1.59	1.61	1.46	2.04
Dy	5.52	9.34	4.38	7.37	7.23	8.67	5.67	7.63	8.36	7.26	9.93
Ho	0.88	1.58	0.81	1.21	1.42	1.56	0.93	1.33	1.48	1.30	1.82
Er	1.82	3.53	1.59	2.67	2.79	3.41	2.26	2.96	3.18	3.00	3.78
Tm	0.20	0.37	0.20	0.28	0.32	0.37	0.25	0.33	0.36	0.35	0.42
Yb	0.96	2.01	1.09	1.58	1.60	1.89	1.21	1.75	1.88	1.83	2.21
Lu	0.11	0.28	0.13	0.18	0.19	0.25	0.13	0.22	0.28	0.23	0.30
Y	22.98	42.49	22.41	30.99	37.00	38.50	29.56	37.92	38.61	38.05	49.27
Total REE	127.93	228.48	124.03	189.84	199.83	225.72	159.27	208.03	209.52	195.42	255.75
La/Sm	1.68	1.82	2.16	1.82	1.89	1.98	2.35	2.36	2.00	2.19	2.11
Eu/Eu*	1.02	0.79	1.14	0.92	0.81	0.87	1.02	1.25	1.11	1.23	1.09
$(La/Yb)_N$	11.21	9.75	10.79	10.47	11.11	10.85	13.40	11.85	10.13	10.23	10.68

3.1. Bulk cumulates composition

Based on major elements, Duchesne and Charlier (2005) have distinguished two major types of cumulates. Following the nomenclature of Irvine (1982) and Wilson et al. (1996), the first group of cumulates globally called "leuconorite" have plagioclase (p), ilmenite (i), Ca-poor pyroxene (h), ±magnetite (m), ±olivine (o) as cumulus minerals (pih-C, pihm-C and pimo-C). The second group named "gabbronorite" is constituted by plagioclase, ilmenite, Ca-poor and Ca-rich pyroxenes (c), magnetite and apatite (a) (pihmac-C). In the upper part of MCU IV, the Ca-poor pyroxene is an inverted pigeonite (h') (pih'mac-C).

REE spectra normalized to chondrites for 22 leuconorites are presented in Fig. 2. Cumulates from different MCUs display similar patterns with a high positive Eu anomaly (Eu/Eu*=2.33 to 11.14) and LREE-enrichment ($(La/Yb)_N$=6.76 to 34.43). REE contents vary significantly, with similar ranges of composition in the different MCU (La=1.64 to 6.50 ppm). Generally, REE-rich samples have smaller Eu anomalies than REE-poor ones.

Fig. 3 displays REE spectra of 12 gabbronorites normalized to chondrites. Three groups were distinguished: pihmac-C of MCU III, those of MCU IV and the pih'mac-C of MCU IV. Gabbronorites are characterized by the coexistence of cumulus apatite and Ca-rich pyroxene. Contrary to leuconorites, they have fairly flat spectra with no or only weak positive or negative Eu anomalies (Eu/Eu*=0.81 to 1.25). The LREE-enrichment is similar in all three groups ($(La/Yb)_N$=9.75 to 13.40). Apatite-bearing cumulates display higher REE contents than leuconorites (La varies from 15 to 32.9 ppm) and their REE patterns are consistently similar to that of typical apatite (see below).

3.2. Mineral compositions

The REE contents of minerals separated from selected cumulates are given in Table 2. Fig. 4

displays ranges of REE content normalized to chondrites for these minerals. Plagioclase patterns show a pronounced LREE-enrichment, a large positive Eu anomaly, and a limited range of composition (La=2.15 to 4.60 ppm). Ca-poor pyroxenes have REE concentrations similar to chondrite with slight HREE-enrichment and, compared to plagioclase, are richer in REE from Dy to Lu. Ca-rich pyroxenes display a domical pattern due to enrichment in middle REE and a very slight negative Eu anomaly. Apatite is clearly the most REE-rich mineral; it is LREE-enriched with a small negative Eu anomaly. Significant variations in apatite composition are observed (La=144 to 344 ppm) with apatites from the most evolved cumulates of MCU IV being the most REE-enriched. Ilmenite and magnetite are REE-poor, with abundances lower than plagioclase for LREE and lower than Ca-poor pyroxene for HREE; they display similar patterns with a LREE-enrichment and no Eu anomaly.

4. Controlling factors on REE distribution in bulk cumulates

4.1. Geostatistical analysis: a first approach

Correlation matrix and principal components analysis have been performed as a first approach to understand the relationships between some REE (La, Ce, Sm, Eu, Gd, Yb), La/Sm, Eu anomaly (Eu/Eu*), $(La/Yb)_N$ and some major elements (Al_2O_3, MgO and P_2O_5). Duchesne and Charlier (2005) have shown that major elements in cumulates display linear trends in variation diagrams. This has been explained by a two-pole cumulate concept. One pole consists exclusively of plagioclase and the other pole comprises all mafic minerals (Ca-poor pyroxene, ilmenite, ±magnetite for leuconorites and two pyroxenes, ilmenite, magnetite and apatite for gabbronorites). These mafic minerals remain essentially in constant proportion for a given type of cumulate. Two factors can thus explain the variation of major elements: Al_2O_3 represents the plagioclase pole and MgO the mafic pole. P_2O_5 has also been selected to express the amount of trapped liquid in leuconorites in which P_2O_5 is incompatible, and the abundance of cumulus apatite in gabbronorites.

The correlations matrices are presented in Table 3. For leuconorites, the most significant results are the good correlation coefficients (r) among the different REE, with an increasing degree of correlation between neighbouring REE. As an example, r between Gd and other REE continuously increase from 0.89 with La to 0.99 with Sm. Eu is better correlated with LREE and has no correlation with Yb ($r=0.03$). La/Sm and Eu/Eu* are negatively correlated with REE. P_2O_5 is well correlated with middle REE (Gd and Sm) with a maximum $r=0.81$ for Sm but less with Yb ($r=0.43$) and Eu ($r=0.41$). Variability in correlation coefficients between the different REE and P_2O_5 immediately imply that the trapped liquid, monitored by P_2O_5 which does not enter into any of the cumulus minerals in leuconorites, does not alone control the REE distribution in these rocks. For gabbronorites, P_2O_5 is, surprisingly, poorly correlated with REE and even negatively correlated with Eu. Nevertheless, all REE, including Eu, are very well correlated with each other ($r=0.72$ to 0.98). La/Sm and Eu/Eu* have a strong negative correlation with P_2O_5. It seems as though a more complex relation is needed between the REE content of bulk gabbronorite cumulates and the amount of cumulus apatite.

In the principal component analysis, factor loadings for leuconorites and gabbronorites (Table 4) have been derived from the correlation matrices. Most of the variation in the data is explained by two principal components, which together account for 99 and 98% of the variance for leuconorites and gabbronorites respectively.

In leuconorites, PC1 (principal component 1) represents 69% of the total variance and is heavily positively loaded by P_2O_5 and the REE and negatively by Al_2O_3 (the plagioclase pole), La/Sm, Eu/Eu* and $(La/Yb)_N$. PC2 (30% of the total variance) essentially displays contrasting behaviour between MgO (the mafic pole) compared to other elements and particularly Al_2O_3 and Eu (the plagioclase pole). Factor loadings are represented in binary diagrams (PC1 vs. PC2) on Fig. 5A. This figure shows that LREE are closer to Al_2O_3 (the plagioclase pole) while HREE and especially Yb are nearer to MgO (the mafic pole). Eu is isolated between the other REE and the plagioclase pole.

In gabbronorites (Fig. 5B), PC1 (76% of the total variance) illustrates the two-pole cumulates concept,

Table 2
REE contents of separated cumulus minerals from selected BKSK cumulates

	Apatite											Orthopyroxene		Clinopyroxene	
Sample No.	00-65	66-74[a]	7969[a]	64-44[a]	64-42	64-43	00-70	66-95[a]	66-102	64-60[a]	66-103[a]	66-74	64-44	66-74	64-44
MCU	III	III	III	IV	IV	IV	IV	IV	IV	IV	IV	III	IV	III	IV
	pihmac-C	pihmac-C	pihmac-C	pihmac-C	pihmac-C	pihmac-C	pihmac-C	pihmac-C	pih'mac-C	pih'mac-C	pih'mac-C	pihmac-C	pihmac-C	pihmac-C	pihmac-C
La (ppm)	205	144	149	216	242	185	169	248	265	344	337	0.1	0.17	1.61	2.46
Ce	614	429	414	606	724	573	520	686	804	947	918	0.22	0.4	6.96	9.97
Pr	90	–	–	–	108	89	79	–	121	–	–	0.04	0.08	1.91	2.77
Nd	499	532	494	479	595	508	443	703	675	652	658	0.2	0.4	11.06	16.57
Sm	99	96.5	95.6	130	116	105	89	146	132	180	175	0.075	0.15	4.38	5.8
Eu	23.6	20.2	19.4	25.9	24.5	24.3	16.3	26.4	31.5	31.4	32.6	0.032	0.048	1.39	1.74
Gd	107	86	85.3	125	136	123	75	124	147	144	173	0.108	0.206	5.64	6.53
Tb	14.1	13.5	11.5	16.1	18.3	14.9	9.3	19.2	18.7	–	23.7	0.03	0.047	0.8	1.09
Dy	62	51.4	53.1	65.3	79	67	40	78.4	82	99.8	94.3	0.254	0.394	4.43	5.97
Ho	11	12.2	9.2	10.3	14.9	12.1	7.1	14.7	15	14.8	21.9	0.068	0.101	0.82	1.11
Er	24.1	22.2	19.8	26.0	32.8	25.2	15.7	33.8	33.0	49.3	43.2	0.222	0.351	1.85	2.56
Tm	2.7	–	–	–	4.1	2.8	1.7	–	3.7	–	–	0.033	0.065	0.23	0.32
Yb	12.1	10.0	9.9	17.8	18.1	11.8	7.5	17.4	16.2	25.0	23.7	0.256	0.452	1.18	1.74
Lu	1.7	1.0	1.0	1.9	3.0	1.7	1.1	2.1	2.3	2.4	2.1	0.039	0.069	0.15	0.21
Total REE[b]	1658.5	1404.5	1350.3	1703.2	1985.3	1636.1	1383.7	2079.8	2203	2489.7	2478.8	1.677	2.933	42.41	58.84
La/Sm	2.1	1.5	1.6	1.7	2.1	1.8	1.9	1.7	2	1.9	1.9	1.3	1.1	0.37	0.42
Eu/Eu*	0.7	0.7	0.7	0.6	0.6	0.7	0.6	0.6	0.7	0.6	0.6	1.09	0.83	0.85	0.86
$(La/Yb)_N$	12.2	10.3	10.8	8.7	9.6	11.2	16.2	10.2	11.7	9.9	10.2	0.28	0.27	0.98	1.01

	Plagioclase									Ilmenite	Magnetite
Sample No.	00-65	66-74	64-44	64-42	64-43	00-70	66-95	66-102	66-103	64-44[c]	64-44[c]
MCU	III	III	IV	IV	IV	IV	IV	IV	IV	IV	IV
	pihmac-C	pihmac-C	pihmac-C	pihmac-C	pihmac-C	pihmac-C	pihmac-C	pih'mac-C	pih'mac-C	pihmac-C	pihmac-C
An[d]	43.1	44.9	47.0	41.7	43.4	45.3	43.7	40.9	39.1	–	–
Or[d]	5.5	4.5	2.4	5.7	4.1	3.1	3.9	5.2	6.1	–	–
P_2O_5 (%)[d]	0.02	0.03	0.02	0.02	0.02	0.01	0.02	0.02	0.02	–	–
La (ppm)	3.31	2.15	2.95	4.21	2.94	3.31	3.54	4.15	4.6	0.74	0.27
Ce	4.74	3.24	5.01	6.38	4.73	4.38	5.39	6.02	6.5	1.81	0.74
Pr	0.65	0.37	0.71	0.62	0.54	0.54	0.54	0.6	0.86	–	–
Nd	1.61	1.34	1.86	1.87	1.62	1.64	2.11	1.99	2.43	0.9	0.5
Sm	0.19	0.25	0.26	0.27	0.27	0.24	0.29	0.23	0.3	0.29	0.1
Eu	1.38	1.26	1.47	1.67	1.72	1.49	2.02	3.42	3.97	0.092	0.03
Gd	0.191	0.208	0.204	0.208	0.235	0.196	0.231	0.195	0.249	–	–
Tb	–	–	–	–	–	–	–	–	–	0.033	0.013
Dy	0.165	0.177	0.187	0.166	0.173	0.175	0.203	0.157	0.221	–	–
Er	0.084	0.092	0.094	0.075	0.072	0.086	0.093	0.077	0.111	–	–
Yb	0.084	0.067	0.084	0.057	0.063	0.067	0.074	0.061	0.094	0.14	0.036
Lu	–	–	0.011	–	–	0.009	0.01	–	0.014	0.033	0.005
Total REE[b]	12.404	9.154	12.829	15.526	12.363	12.124	14.491	16.9	19.335	–	–
La/Sm	17.4	8.6	11.3	15.6	10.9	13.8	12.2	18.0	15.3	2.6	2.7
Eu/Eu*	22.3	17.0	19.7	21.7	21.1	21.2	24.1	49.8	44.8	–	–
$(La/Yb)_N$	25.5	17.4	22.7	47.8	30.2	35.4	31.0	44.0	31.7	3.8	5.4

[a] Roelandts and Duchesne (1979).
[b] Except Pr, Tb and Tm.
[c] From Roelandts (1975).
[d] From major elements by XRF.

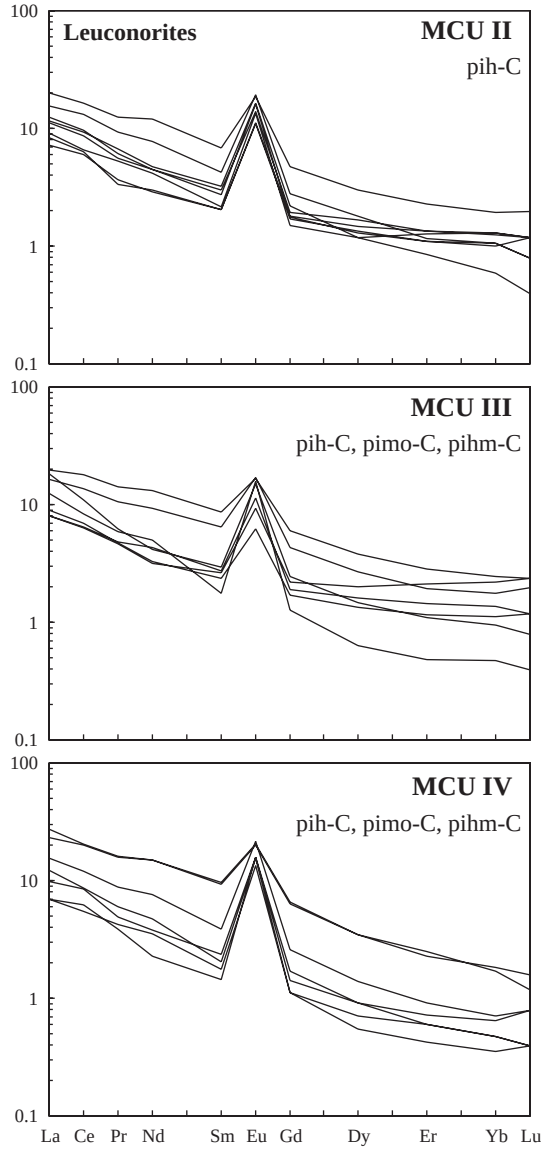

Fig. 2. REE patterns normalized to chondrites (Sun and McDonough, 1989) for bulk leuconoritic cumulates of MCU II, III and IV. Mineral abbreviations are p—plagioclase, i—ilmenite, h—Ca-poor pyroxene, m—magnetite, o—olivine.

with the plagioclase pole (Al_2O_3) associated with Eu/Eu*, La/Sm and $(La/Yb)_N$ opposite the mafic pole (MgO and P_2O_5) with which REE are correlated. PC2 (22% of the total variance) is negatively loaded by MgO and P_2O_5, and positively by other variables, especially Eu. In this case, middle REE (here Sm) have a better correlation with P_2O_5 than other REE (La and Yb).

It can be concluded from this geostatistical analysis that the REE distribution in bulk cumulates is controlled by a variety of parameters. Even if REE are clearly associated with P_2O_5, which represents the

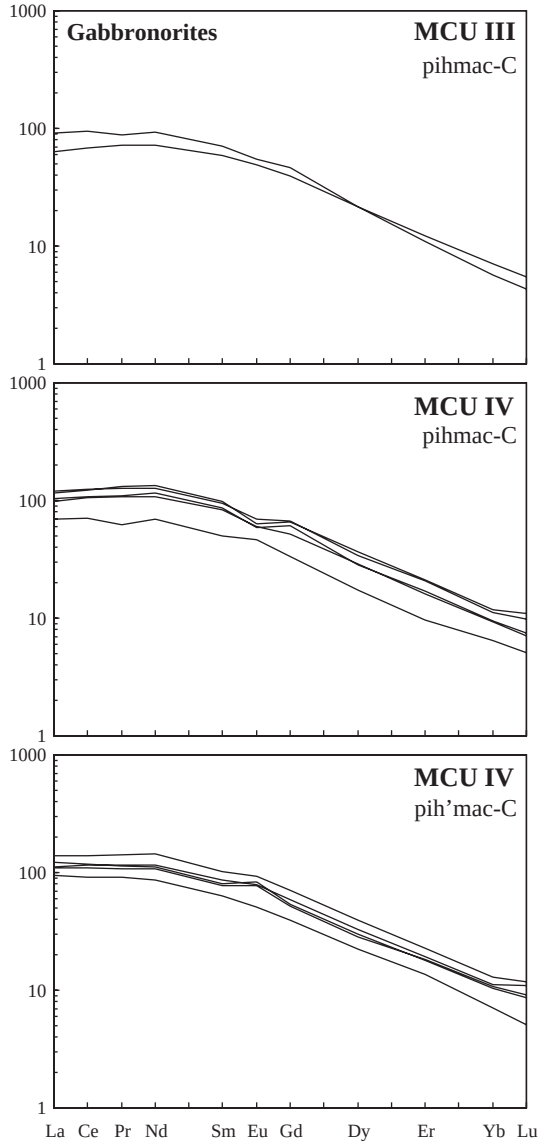

Fig. 3. REE patterns normalized to chondrites (Sun and McDonough, 1989) for bulk gabbronoritic cumulates of MCU II, III and IV. Mineral abbreviations are p—plagioclase, i—ilmenite, h—Ca-poor pyroxene, m—magnetite, a—apatite, c—Ca-rich pyroxene, h′—inverted pigeonite.

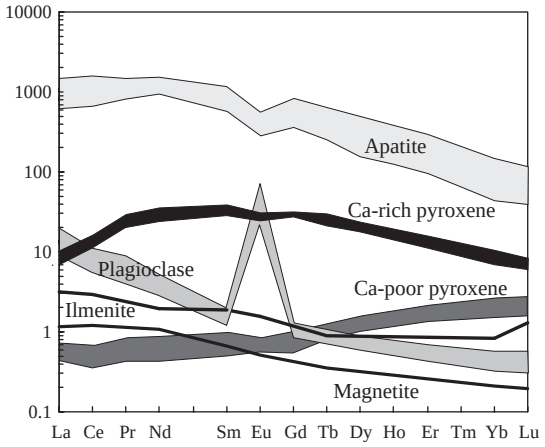

Fig. 4. Ranges of REE content normalized to chondrites (Sun and McDonough, 1989) for plagioclase, Ca-poor and Ca-rich pyroxenes, apatite, ilmenite and magnetite.

amount of trapped liquid in leuconorites or the modal abundance of cumulus apatite in gabbronorites, cumulus minerals which are represented by the plagioclase pole and the mafic pole also act as controlling factors on REE distribution. In leuconorites, LREE and HREE display contrasting behaviour. LREE (including Eu) are better correlated with plagioclase whereas HREE are correlated with the mafic pole. This emerges from the cumulus minerals spectra; plagioclase is LREE-enriched and Ca-poor pyroxene is HREE-enriched. In gabbronorites, the mafic pole includes cumulus apatite. This explains the correlation between MgO and P_2O_5. In these cumulates, the two-pole cumulate concept of Duchesne and Charlier (2005) thus accounts for most of the variability.

4.2. Leuconorite geochemistry

It appears from Fig. 2 that REE patterns for leuconorites retain essentially the same shape, except for the size of the Eu anomaly. Nevertheless, the bulk REE content varies significantly (Ce varies from ~3 to ~12 ppm), even for cumulates with approximately the same major element concentrations, i.e., the same modal proportion of cumulus minerals (see Table 1). Variability of the REE content of cumulus minerals is not responsible for these variations because, as illustrated by plagioclase composition (Table 2), the REE content and range of variation remain low. It is thus insufficient to explain the broad interval of REE concentration in the bulk cumulates. Actually, mass balance calculations show that the whole-rock REE contents in leuconorites do not simply result from mixture between cumulus plagioclase and Ca-poor pyroxene, as is clear from the total REE vs. P_2O_5 content (Fig. 6). The role of oxides can be neglected, as the LREE are controlled by plagioclase and the HREE by Ca-poor pyroxene (Fig. 4). Fig. 6 shows a broad positive correlation between the total REE and the P_2O_5 content, as already demonstrated by the geostatistical analysis. P_2O_5 is not abundant in cumulus minerals (between 0.01 and 0.03% in plagioclase and ~0% in Ca-poor pyroxene), but occurs as interstitial apatite, that crystallized from trapped liquid. The trend in Fig. 6 points towards the jotunite composition (Table 1), which can be considered to have a composition close to the trapped magma. Note the higher scattering of the data at low P_2O_5 values, demonstrating the dominant role of variations of cumulus minerals proportions for low TLF, and of the trapped liquid content for higher P_2O_5 content. A rough estimation of the TLF varies between 0 and 25% with systematic higher values (10–25%) in samples from the north-eastern part of the intrusion (Teksevatnet area), while the TLF in samples from other localities remains below 10%.

Another interesting point is the variation of the positive Eu anomaly in the bulk leuconorite cumulates (Fig. 2). The extent of this anomaly depends on plagioclase and trapped liquid compositions and proportions. Anomalies as weak as 2.33 (00-63) or 2.56 (00-67) compared to values up to 11.1 (64–20b) (Table 1) can only be explained by the presence in the first two samples of interstitial apatite crystallized from the trapped liquid. Indeed, the flat patterns and the much higher REE content of apatite in the trapped melt swamp the whole-rock positive Eu anomaly, controlled by plagioclase. This explains why, in the principal components analysis of leuconorites (Fig. 5A), Eu is isolated relatively close to the plagioclase pole and some distance from other REE and P_2O_5. Trapped liquid can thus affect REE patterns of cumulates, but it is not the only factor to govern the distribution of REE, the latter being also clearly influenced by the compositions of cumulus minerals.

4.3. Gabbronorite geochemistry

As the REE content of apatite is about 100 times higher than that of the other cumulus minerals (Fig. 4), cumulus apatite exerts a major control on the REE patterns and bulk contents of gabbronorites. To demonstrate this, simple calculations can be made (Table 5, Fig. 7) with the compositions of separated minerals of sample 64–44 (Table 2). We fix the proportion of apatite at 5% (weight percent), which is close to the lowest apatite content encountered in gabbronorite, and calculate the composition of theoretical cumulates with various proportions of plagioclase, Ca-poor and Ca-rich pyroxenes (respectively 65, 20, 10% in model 1; 55, 25, 15% in model 2; 45, 30, 20% in model 3 and 35, 30, 30% in model 4). Calculated REE contents of these bulk cumulates are grossly similar, demonstrating that even for significant variations of the modal proportions of plagioclase, Ca-

Table 4
Factor loadings for leuconorites and gabbronorites of the principal components (PC1 and PC2)

Leuconorites			Gabbronorites		
	PC1	PC2		PC1	PC2
Al_2O_3	−0.53	0.84	Al_2O_3	−0.99	0.15
MgO	0.51	−0.85	MgO	0.94	−0.34
P_2O_5	0.90	0.38	P_2O_5	0.88	−0.47
La	0.85	0.51	La	0.83	0.53
Ce	0.90	0.44	Sm	0.98	0.18
Sm	0.97	0.26	Eu	0.60	0.80
Eu	0.34	0.93	Gd	0.98	0.18
Gd	0.98	0.21	Yb	0.90	0.43
Yb	0.96	−0.29	La/Sm	−0.75	0.62
La/Sm	−0.97	0.16	Eu/Eu*	−0.75	0.65
Eu/Eu*	−0.99	0.13	$(La/Yb)_N$	−0.91	−0.18
$(La/Yb)_N$	−0.72	0.68	Variance	8.36	2.37
Variance	8.26	3.59	Proportion	0.76	0.22
Proportion	0.69	0.30	Cumulative proportion	0.76	0.98
Cumulative proportion	0.69	0.99			

Table 3
Correlation matrix for selected whole-rock major elements and REE for leuconorites and gabbronorites of BKSK

	Al_2O_3	MgO	P_2O_5	La	Ce	Sm	Eu	Gd	Yb	La/Sm	Eu/Eu*	$(La/Yb)_N$
Leuconorites												
Al_2O_3	1.00	–	–	–	–	–	–	–	–	–	–	–
MgO	–0.93	1.00	–	–	–	–	–	–	–	–	–	–
P_2O_5	0.14	−0.16	1.00	–	–	–	–	–	–	–	–	–
La	0.25	−0.20	0.72	1.00	–	–	–	–	–	–	–	–
Ce	0.20	−0.15	0.77	0.97	1.00	–	–	–	–	–	–	–
Sm	0.00	0.03	0.81	0.90	0.96	1.00	–	–	–	–	–	–
Eu	0.65	−0.59	0.41	0.72	0.73	0.59	1.00	–	–	–	–	–
Gd	−0.07	0.09	0.79	0.89	0.95	0.99	0.56	1.00	–	–	–	–
Yb	−0.62	0.59	0.43	0.47	0.56	0.70	0.03	0.73	1.00	–	–	–
La/Sm	0.42	−0.38	−0.51	−0.28	−0.45	−0.63	−0.08	−0.63	−0.72	1.00	–	–
Eu/Eu*	0.45	−0.41	−0.61	−0.56	−0.61	−0.73	−0.02	−0.75	−0.83	0.77	1.00	–
$(La/Yb)_N$	0.79	−0.66	0.02	0.19	0.08	−0.11	0.44	−0.17	−0.65	0.65	0.53	1.00
Gabbronorites												
Al_2O_3	1.00	–	–	–	–	–	–	–	–	–	–	–
MgO	−0.95	1.00	–	–	–	–	–	–	–	–	–	–
P_2O_5	−0.78	0.87	1.00	–	–	–	–	–	–	–	–	–
La	−0.53	0.30	0.17	1.00	–	–	–	–	–	–	–	–
Ce	−0.62	0.41	0.30	0.98	1.00	–	–	–	–	–	–	–
Sm	−0.79	0.63	0.56	0.89	0.95	1.00	–	–	–	–	–	–
Eu	−0.28	0.01	−0.11	0.88	0.85	0.73	1.00	–	–	–	–	–
Gd	−0.77	0.61	0.56	0.88	0.93	0.99	0.72	1.00	–	–	–	–
Yb	−0.65	0.43	0.27	0.94	0.96	0.93	0.87	0.92	1.00	–	–	–
La/Sm	0.48	−0.58	−0.75	0.29	0.13	−0.17	0.30	−0.18	0.07	1.00	–	–
Eu/Eu*	0.66	−0.81	−0.91	0.02	−0.10	−0.34	0.39	−0.34	−0.03	0.66	1.00	–
$(La/Yb)_N$	0.52	−0.42	−0.29	−0.25	−0.35	−0.48	−0.37	−0.48	−0.57	0.46	0.08	1.00

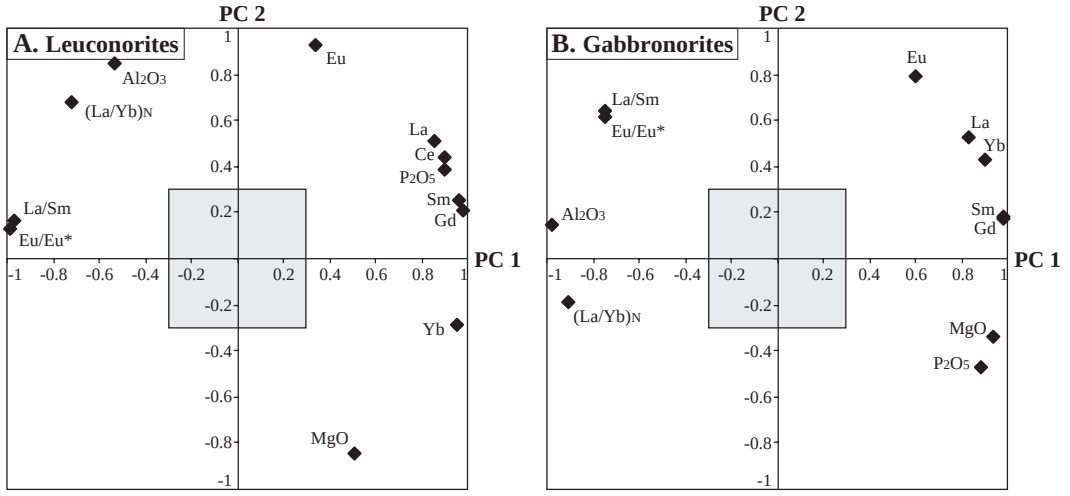

Fig. 5. Graphical representation of the factor loading in the plane of the principal components PC1 and PC2 for (A) leuconorites and (B) gabbronorites.

poor and Ca-rich pyroxenes, the shape of REE spectra remains constant and similar to apatite spectra. It is thus clear that apatite has a buffering role on REE distribution in gabbronorites. We have previously shown that in the principal components analysis, REE are not correlated with P_2O_5, which represents the amount of cumulus apatite. This paradoxical observation is simply due to the cryptic variations of apatite composition (total REE = 1350 to 2489 ppm; Table 2). Finally, bulk gabbronoritic cumulates (Table 1) have nearly the same REE content as the evolved jotunite with which they are in equilibrium (Vander Auwera et al., 1998b). The latter have REE contents which do not vary much in the course of fractionation due to the presence of apatite in the subtracted cumulate. It can thus be concluded that the trapped liquid in gabbronorites, which should be close to the composition of an evolved jotunite, has a REE content similar to that of the sum of cumulus minerals. The influence of the trapped liquid thus cannot be sorted out from that of cumulus apatite.

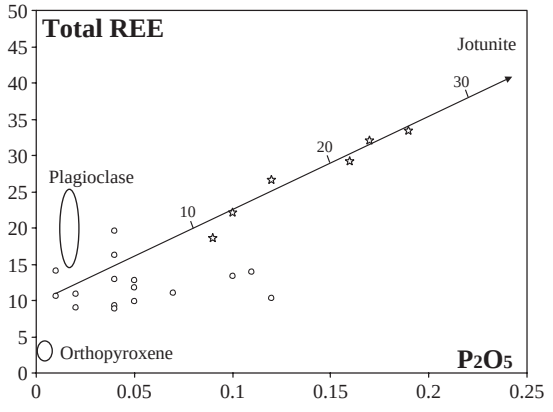

Fig. 6. Total REE vs. P_2O_5 in leuconorites with ranges of composition for plagioclase and orthopyroxene (Table 2), and a rough estimation of the trapped liquid fraction (weight percent) on the mixing line with the jotunite composition from Table 1 (Duchesne and Hertogen, 1988). *Stars* are samples from the north-eastern part (Teksevatnet area) and *open circles* are from other localities.

5. Constraints on the trapped liquid fraction

As shown above, the composition and abundance of cumulus apatite buffer the REE patterns and bulk content in the gabbronorites, whereas in the leuconorites, the trapped liquid fraction (TLF) partly controls the REE behaviour. This property enables us to estimate the TLF only in this type of rock. In Fig. 8, for large variations of P_2O_5, gabbronorites display restricted variations in La/Sm (1.68 to 2.36) and Eu/Eu* (0.79 to 1.25). These variations are in the range of apatite compositions for La/Sm (1.5 to 2.1) and slightly higher than the apatite Eu/Eu* (0.57 to 0.70) due to the contribution of the large positive Eu anomaly of plagioclase. Moreover, La/Sm (~2 to 3)

and Eu/Eu* (~1) of evolved jotunites are similar to the range of variation of the gabbronorites (Vander Auwera et al., 1998b). Leuconorites display contrastingly large ranges in La/Sm (3.57 to 10.89) and Eu/Eu* (2.33 to 10.62) without overlapping jotunite compositions. The compositional variability of leuconorites is modelled in Fig. 9A–B by assuming that it results from the mixing between a pure adcumulate, made up of plagioclase and a mafic pole (Ca-poor pyroxene+oxides), and a primitive jotunite (see Table 6 for the composition of the two end-members). Sample 80.12.3a (Tjörn) which is a chilled margin of BKSK (P_2O_5=0.71%, Duchesne and Hertogen, 1988) has been taken as the reference for the liquid composition, as it has been shown to be a plausible parental magma composition for this intrusion (Duchesne and Hertogen, 1988; Vander Auwera and Longhi, 1994). A second mixing line with a jotunite containing 1% P_2O_5 has also be drawn to show the negligible influence of the liquid composition for trapped liquid

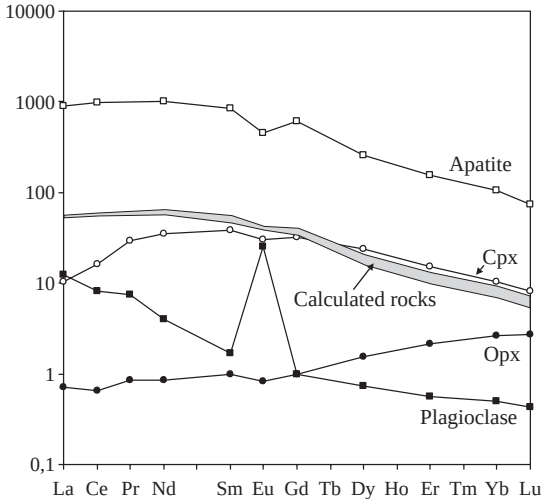

Fig. 7. Illustration of the buffering role of apatite on the REE patterns of gabbronorites. Theoretical rock compositions have been calculated with mineral compositions from sample 64-44 (Table 2). Modal abundances and compositions of calculated rocks are reported in Table 5. REE patterns are normalized to chondrites (Sun and McDonough, 1989).

Table 5
Calculated compositions for 4 hypothetical bulk cumulates using various modal proportions of cumulus minerals (plagioclase, Ca-poor, Ca-rich pyroxenes and apatite) with mineral compositions of sample 64-44 (Table 2)

	Model 1	Model 2	Model 3	Model 4
Modal proportions (weight percent)				
Plagioclase	0.65	0.55	0.45	0.35
Ca-poor pyroxene	0.20	0.25	0.30	0.30
Ca-rich pyroxene	0.10	0.15	0.20	0.30
Apatite	0.05	0.05	0.05	0.05
Calculated REE content of the bulk cumulate (ppm)				
La	13.0	12.8	12.7	12.6
Ce	34.6	34.7	34.7	35.2
Pr	–	–	–	–
Nd	26.9	27.6	28.2	29.7
Sm	7.3	7.6	7.8	8.4
Eu	2.4	2.4	2.3	2.3
Gd	7.1	7.4	7.7	8.3
Tb	0.92	0.98	1.04	1.15
Dy	4.1	4.4	4.7	5.2
Ho	0.65	0.71	0.77	0.88
Er	1.7	1.8	2.0	2.2
Tm	–	–	–	–
Yb	1.21	1.31	1.41	1.58
Lu	0.14	0.15	0.16	0.18
La/Sm	1.79	1.70	1.62	1.51
Eu/Eu*	1.04	0.97	0.91	0.86
$(La/Yb)_N$	7.71	7.03	6.44	5.74

content up to 25%. In this modelling, the theoretical adcumulate with 0% TLF has a low P_2O_5 content (0.02%), mainly accounted for by cumulus plagioclase. Consequently, low values for La, Eu and Sm have been selected (respectively 2.64, 0.95 and 0.22 ppm). These values correspond to an adcumulate with about 70% plagioclase and 30% of mafics minerals, which is close to the average leuconorite (Duchesne and Charlier, 2005). La/Sm and Eu/Eu* for the theoretical adcumulate are slightly higher than for the natural cumulates with the lowest TLF, because interstitial apatite is observed in all rocks, testifying that no cumulate has 0% trapped liquid. The modelling (Fig. 9A and B) shows that the compositional variability of leuconorites can be accounted for by addition of 2% to 25%. Samples from the north-eastern part of the intrusion (Teksevatnet area) have globally higher TLF (10–25%) and, following Irvine (1982), can be considered as mesocumulates. The TLF in other samples varies between 2 and 10%. They are closer to the range of adcumulates. The existence of these two contrasted types of cumulates, in two different localities, probably results from different thermal regime. The cooling rate was slightly greater in the Teksevatnet area producing more orthocumulate-like textures, now obscured by the subsequent deformation, and only detected geochemi-

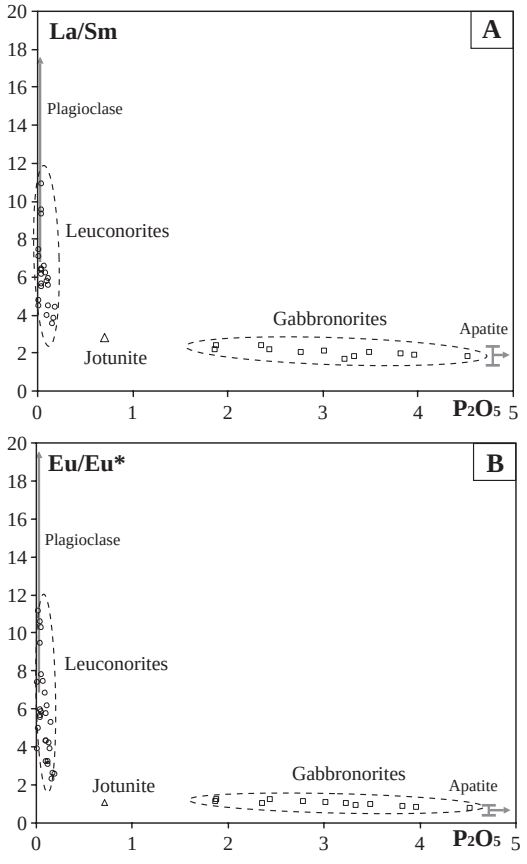

Fig. 8. (A) La/Sm vs. P_2O_5 and (B) Eu/Eu* vs. P_2O_5 for bulk cumulates (leuconorites—*open circles* (○) and gabbronorites—*open squares* (□)) and jotunite—*open triangle* (△) with the range of composition for plagioclase and apatite indicated by the arrow.

cally by the greater proportion of trapped liquid. This certainly results from the location on the flank, where the gneissic country rock floor was relatively closer to crystallizing cumulates in this part of the intrusion, compared with the main part of the layered series where underlying cumulates were thicker (J.R. Wilson, personal communication).

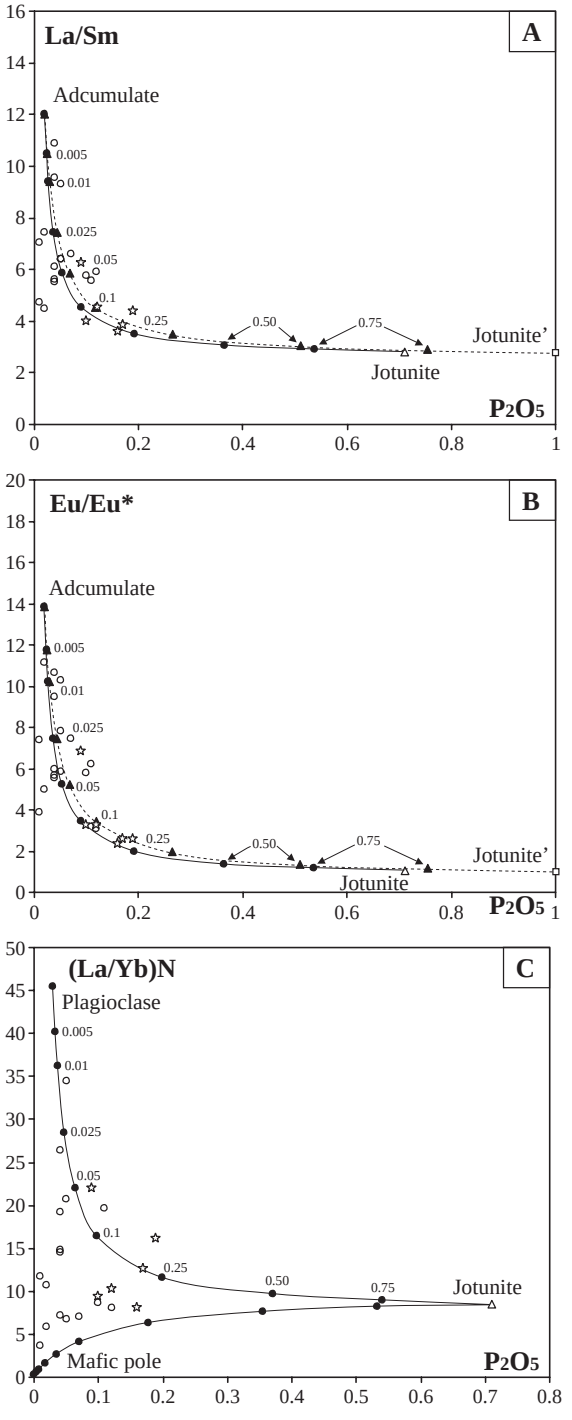

Fig. 9. (A) La/Sm vs. P_2O_5 and (B) Eu/Eu* vs. P_2O_5 for leuconorites and jotunite with mixing lines between bulk adcumulate and jotunite with the relative percentage of jotunite. Jotunite (△) is the proposed parental magma of BKSK (Duchesne and Hertogen, 1988) and Jotunite' (□) has the same REE content with 1% P_2O_5 (see Table 6). (C) $(La/Yb)_N$ vs. P_2O_5 for leuconorites with mixing lines plagioclase–jotunite and orthopyroxene–jotunite with the relative percentage of jotunite. *Stars* are samples from the north-eastern part (Teksevatnet area) and *open circles* (○) are from other localities.

Table 6
Composition for end-members of mixing models of leuconorite cumulates

	Jotunite[a]	Jotunite[b]	Theoretical adcumulate[c] with 0% TLF	Plag	Mafic pole
P_2O_5	0.71	1.00	0.02	0.03	0
La	23.9	23.9	2.64	3.8	0.1
Sm	8.5	8.5	0.22	–	–
La/Sm	2.8	2.8	12	–	–
Eu	2.86	2.86	0.95	–	–
Eu/Eu[a]	1.06	1.06	13.85	–	–
Yb	2	2	–	0.06	0.26
$(La/Yb)_N$	8.6	8.6	–	45.4	0.28

[a] Sample Tjørn from Duchesne and Hertogen (1988).
[b] Jotunite' has 1% P_2O_5 to show the negligible influence of the parental magma composition for low trapped liquid fractions.
[c] This composition corresponds to a cumulate with 70% plagioclase and 30% low-Ca pyroxene+ilmenite.

This modelling gives a good estimate of the TLF even if we have considered only one pure adcumulate pole, with a single modal proportion of cumulus minerals, and approximated that cumulus minerals and trapped liquid have a constant composition. Indeed, the La/Sm and Eu/Eu* ratios are essentially controlled by plagioclase, which has a large Eu anomaly and is the LREE-richest cumulus mineral in leuconorite, but these ratios are also influenced by the relative proportion of Ca-poor pyroxene and oxides which have a low La/Sm (~1 to 3) and thus have a diluting effect on the bulk composition. This can explain the scattering observed around the mixing line and can be illustrated by plotting the $(La/Yb)_N$ ratio vs. P_2O_5 (Fig. 9C). This ratio is very sensitive to the relative amount of cumulus plagioclase and mafic minerals (Ca-poor pyroxene+oxides) since plagioclase is LREE-enriched and the mafics are HREE-enriched. In this diagram, almost all the cumulates plot between the two mixing curves of plagioclase–jotunite and mafic minerals–jotunite.

6. Trace elements modelling: reconstruction of liquid composition

6.1. Methodology

The reconstruction of trace elements compositions of liquids in equilibrium with the BKSK cumulates is investigated through a mass balance calculation. This method, called the equilibrium distribution method (EDM) by Bédard (1994, 2001), was first proposed by Cawthorn et al. (1991) to model the REE abundances of parental liquid to the Main Zone of the Bushveld Complex.

Liquids can be reconstructed if one knows the bulk cumulate trace elements contents, the weight proportion of the cumulus minerals, the trapped liquid fraction (TLF) and a set of partition coefficients. Using these data, it is possible to calculate the trace element content of cumulus minerals assuming that equilibrium prevails between them and that the trapped liquid has crystallized as a closed-system. The calculation ends up with the composition of the liquid from which these cumulates have crystallized by inversion with partition coefficients. Equations developed in Bédard (1994, 2001) are applied in this work. By mass balance, and taking the example of a leuconorite with plagioclase (p), Ca-poor pyroxene (h), ilmenite (i) and trapped liquid (tl) with their respective weight modal proportion (ϕ), the bulk composition of the leuconorite can be expressed as:

$$C_j^{\text{rock}} = \left(\phi^{\text{p}} C_j^{\text{p}}\right) + \left(\phi^{\text{h}} C_j^{\text{h}}\right) + \left(\phi^{\text{i}} C_j^{\text{i}}\right) + \left(\phi^{\text{tl}} C_j^{\text{tl}}\right) \quad (1)$$

As we know, the content of the element j in the bulk cumulate (C_j^{rock}) and the modal proportion of the cumulus minerals which has been determined by point counting and corrected for the mode of the trapped liquid (the normative proportion of the jotunite), it is possible to calculate the trace element content of each mineral and of the trapped liquid. Knowing that the partition coefficient ${}^{\text{min/liq}}D_j = C_j^{\text{min}}/C_j^{\text{liq}}$, and that ${}^{\text{tl/liq}}D_j = 1$, we deduce that:

$$C_j^{\text{p}} = C_j^{\text{h}}\left({}^{p/liq}D_j / {}^{h/liq}D_j\right) = C_j^{\text{i}}\left({}^{p/liq}D_j / {}^{i/liq}D_j\right) \quad (2)$$

By substituting Eq. (2) in (1), we obtain:

$$C_j^{\text{p}} = C_j^{\text{rock}} \Big/ \left(\phi^{\text{p}} + \phi^{\text{h}} \frac{{}^{h/liq}D_j}{{}^{p/liq}D_j} + \phi^{\text{i}} \frac{{}^{i/liq}D_j}{{}^{p/liq}D_j} + \frac{\phi^{\text{tl}}}{{}^{p/liq}D_j}\right) \quad (3)$$

The compositions of the other minerals can be solved similarly. The composition of the liquid with

which these minerals are in equilibrium can then be calculated using their respective partition coefficients. The crucial interest of this modelling is that it takes into account the TLF. Conversely, if the composition of liquids in equilibrium with cumulates is known, it is possible to constrain the TLF. This property will be discussed below.

6.2. Partition coefficients

The application of the EDM requires a set of appropriate partition coefficients. These are classically compiled from the literature but, in our particular case, as jotunitic liquids are rather scarce and as D's depend on crystallization temperature, on mineral compositions and, as shown by Vander Auwera et al. (2000), for some of them on pressure, we have used the following approach.

Duchesne and Charlier (2005) have calculated the fraction of liquid ($F=0.6$) residual after the crystallization of the leuconoritic cumulates. Their result is in broad agreement with previous estimates by Duchesne (1978) ($F=0.47$) and by Vander Auwera et al. (1998b) ($F=0.5$). REE in the leuconoritic stage are incompatible and the liquid composition (C_{liq}) thus follows the simplified Rayleigh equation $C_{liq}=C_0/F$ where C_0 is the concentration in the parental magma. Considering that the primitive jotunite of Duchesne and Hertogen (1988), with La=23.9 ppm, is the BKSK parental magma, the composition of the liquid C_{liq} will be La=39.8 ppm at the end of the leuconoritic stage for $F=0.6$. At that time, apatite first appears as a cumulus mineral. As $D_j^{apatite}=(C_j^{apatite}/C_j^{liq})$, the most primitive apatite can be used to calculate the partition coefficient between apatite and liquid. The three apatites with the lowest REE contents (66-74, 7969 and 00-70) which come from cumulates situated stratigraphically near the base of the gabbronoritic cumulates have been selected for this calculation in order to minimize the analytical uncertainty (Table 7). The major element composition of the melt in equilibrium with apatites corresponds to the evolved jotunite L2 of Duchesne and Charlier (2005). These calculated partition coefficients for REE between apatite and liquid are analogous to those previously calculated by Roelandts and Duchesne (1979) for BKSK, and remarkably similar to those obtained experimentally by Watson and Green (1981) with a tholeiitic andesite composition, not significantly different from a jotunite composition.

As partition coefficients between apatite and liquid are known and the REE content of cumulus minerals has been analysed in some samples (Table 2), the REE distribution between minerals can be used to calculate

Table 7
REE composition for the parental liquid (C_0) and the liquid at the end of the leuconoritic stage for $F=0.6$ (C_{liq}) and partition coefficients for REE between this liquid and 3 apatites

	80.12.3a[a] Jotunite C_0	$C_{liq}=C_0/F$ (with $F=0.6$)	66-74 Apatite	7969 Apatite	00-70 Apatite	D_i 66-74	D_i 7969	D_i 00-70	D_i Average (s)	Watson and Green (1981) Run 812
La	23.9	39.8	144	149	169	3.6	3.7	4.2	3.8 (0.3)	3.4 (0.5)
Ce	58	96.7	429	414	520	4.4	4.3	5.4	4.7 (0.6)	
Pr	–	–	–	–	79					
Nd	39	65.0	532	494	443	8.2	7.6	6.8	7.5 (0.7)	
Pr	–	–	–	–	–					
Sm	8.5	14.2	96.5	95.6	89	6.8	6.7	6.3	6.6 (0.3)	7.8 (1.1)
Eu	2.86	4.8	20.2	19.4	16.3	4.2	4.1	3.4	3.9 (0.4)	
Gd	–	–	86	85.3	75					
Tb	1.13	1.88	13.5	11.5	9.3	7.2	6.1	4.9	6.1 (1.2)	
Dy	–	–	51.4	53.1	40					5.4 (0.6)
Ho	–	–	12.2	9.2	7.1					
Er	–	–	22.2	19.8	15.7					
Tm	–	–	–	–	1.7					
Yb	2.00	3.33	10.0	9.9	7.5	3.0	3.0	2.3	2.8 (0.4)	
Lu	–	–	1.0	1.0	1.1					2.9 (0.3)

Average values are compared to experimental data of Watson and Green (1981). s—Standard deviation.
[a] Duchesne and Hertogen (1988).

partition coefficients for the other cumulus minerals. These can be calculated thus: for element j,

$$D_j^{\min 1} = \frac{C_j^{\min 1}}{C_j^{\mathrm{liq}}} \frac{C_j^{\min 2}}{C_j^{\min 2}} = D_j^{\min 2} D_j^{\min 1/\min 2}$$

Nine pairs of plagioclase–apatite have been used to calculate partition coefficients for plagioclase, 2 pairs for Ca-poor and Ca-rich pyroxenes and 1 pair for ilmenite and magnetite. Average values and standard deviations are reported in Table 8. Values for D_{REE} of olivine have been selected from the literature (Dunn and Sen, 1994) as olivine was not analysed for REE.

In this procedure, we assume that mineral compositions have retained their high-temperature magmatic signatures, i.e., that reequilibration with trapped liquid (Cawthorn, 1996) or as a result of postcumulus phenomena such as fluid transfer (Irvine, 1980; Meurer et al., 1997) did not occur. Indeed, in the gabbronoritic cumulates selected for this calculation, apatite is a cumulus mineral and, as already shown above, the REE content of cumulus minerals is not affected by the trapped liquid because the latter has a composition close to the cumulate composition and apatite absorbs the major part of trapped liquid REE. The overgrowth part of the other cumulus minerals will thus not be enriched in these elements. Moreover, Duchesne and Wilmart (1997) have shown that liquids from the upper part of BKSK have very low H_2O contents, minimizing the possibility of any postcumulus fluid transfer. This hypothesis is corroborated by the broadly anhydrous mineralogy of BKSK rocks and by the lack of late-stage veins, pegmatitic facies, metasomatic replacement or discordant bodies.

6.3. Application to BKSK cumulates

The most primitive cumulates of BKSK are present at the base of each MCU, where new, undifferentiated magma entered the chamber. Troctolitic cumulates (pimo-C) situated near the base of MCU IV contain the most primitive mineral assemblages in BKSK (olivine Fo75-62; plagioclase An53-48, chromium-rich magnetite and ilmenite) (Duchesne, 1972; Nielsen and Wilson, 1991; Jensen et al., 1993). These cumulates should have been in equilibrium with the most primitive liquid which is taken as being identical to the jotunite parental magma of the intrusion described by Duchesne and Hertogen (1988) and Vander Auwera and Longhi (1994). Based on this assumption, the TLF can be adjusted in order to obtain a calculated liquid similar to the parental magma. The EDM has been applied to the four pimo-C cumulates from the base of MCU IV (00-67, 00-71, 00-73 and

Table 8
Calculated REE partition coefficients (mineral/jotunite) for the application of the equilibrium distribution method

	Plagioclase		Ca-poor pyroxene		Apatite		Ca-rich pyroxene		Ilm	Mag	Olivine[a]
	D_i	s	D_i	s	D_i	s	D_i	s	D_i	D_i	D_i
La	0.061	(0.007)	0.003	(0.000)	3.9	(0.3)	0.044	(0.001)	0.013	0.005	0.003
Ce	0.037	(0.003)	0.003	(0.000)	4.7	(0.6)	0.077	(0.001)	0.014	0.006	0.004
Pr	0.033	(0.005)	–	–	*5.4*	–	–	–	*0.013*	–	0.005
Nd	0.020	(0.003)	0.004	(0.002)	*6*	–	0.166	(0.059)	0.011	0.006	0.01
Sm	0.014	(0.003)	0.006	(0.002)	6.6	(0.3)	0.297	(0.004)	0.015	0.005	0.02
Eu	0.310	(0.090)	0.007	(0.001)	3.9	(0.4)	0.265	(0.004)	0.014	0.005	0.02
Gd	0.013	(0.003)	0.010	(0.002)	*6.8*	–	0.401	(0.064)	*0.014*	*0.005*	0.03
Tb	–	–	–	–	6.1	(1.2)	–	–	0.013	0.005	0.035
Dy	0.014	(0.004)	0.029	(0.004)	*5.3*	–	0.471	(0.020)	*0.014*	*0.005*	0.034
Ho	–	–	–	–	*4.6*	–	–	–	–	–	0.037
Er	0.013	(0.004)	0.047	(0.010)	*4*	–	0.364	(0.043)	*0.017*	*0.005*	0.04
Tm	–	–	–	–	*3.4*	–	–	–	–	–	0.04
Yb	0.013	(0.004)	0.069	(0.000)	2.7	(0.4)	0.291	(0.039)	0.021	0.005	0.05
Lu	0.013	(0.002)	0.083	(0.004)	*2.2*	–	0.287	(0.061)	*0.025*	0.006	0.05

s—Standard deviation. Values in italics have been extrapolated.
[a] Dunn and Sen (1994).

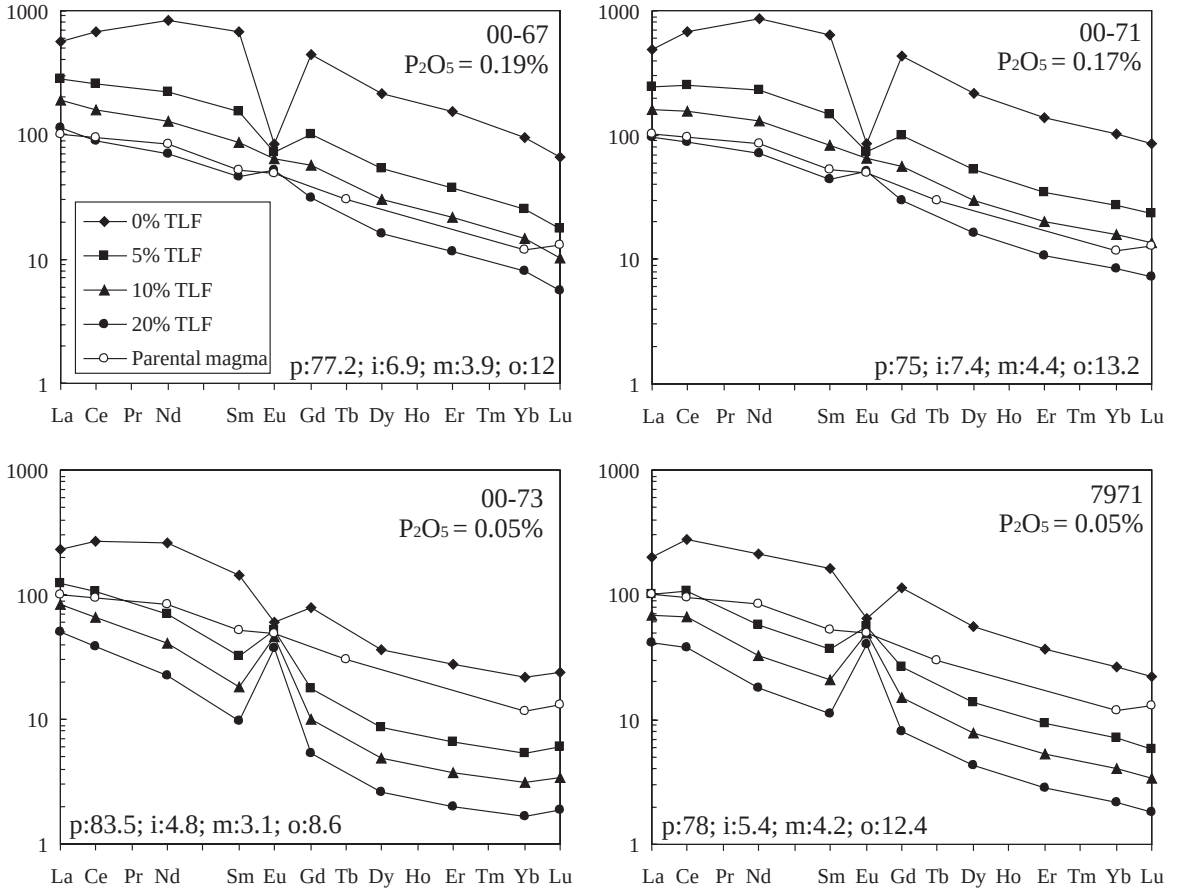

Fig. 10. REE composition of calculated liquids with the EDM (data normalized to chondrites, Sun and McDonough, 1989) for trapped liquid fraction (TLF) of 0, 5, 10 and 20% for four troctolitic (pimo-C) cumulates of MCU IV (with their modal proportion of cumulus minerals in weight percent and the P_2O_5 content of the bulk cumulate), and composition of the jotunitic parental magma (Duchesne and Hertogen, 1988).

7971) which have different P_2O_5 contents (0.19, 0.17, 0.05 and 0.05% respectively). Liquid compositions have been calculated for various TLF (0, 5, 10 and 20%) and are reported on Fig. 10. They are similar to the jotunite parental magma for TLF around 20% for samples 00-67 and 00-71. This is consistent with their P_2O_5 contents which reflect TLFs of 24% and 21% respectively, assuming 0.71% P_2O_5 in the trapped liquid and corrected for the 0.02% present in cumulus minerals. For samples 00-73 and 7971, calculated liquids are similar to the jotunite parental magma for TLF lower than 5%. Their P_2O_5 content is also lower (0.05%) and corresponds to a TLF of 4%.

These examples illustrate that the composition of calculated liquids in equilibrium with cumulates without cumulus apatite is extremely sensitive to

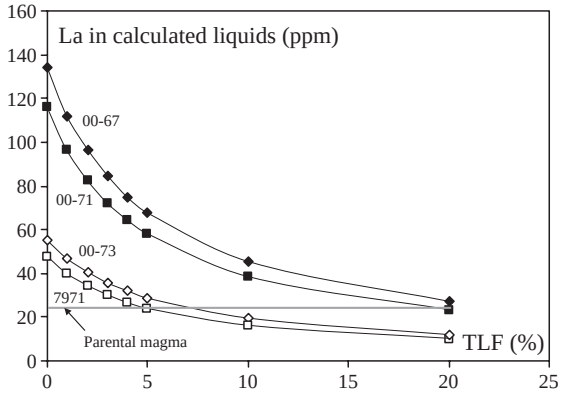

Fig. 11. La content of calculated liquids vs. the trapped liquid fraction (TLF) for four troctolitic (pimo-C) cumulates near the base of MCU IV. The horizontal grey line represents the composition of the jotunitic parental magma (Duchesne and Hertogen, 1988).

the TLF. This is shown on Fig. 11 where the composition of the calculated liquid (the La content) is expressed as a function of the TLF. It emerges that a TLF lower than 5% significantly influences the composition of the calculated liquid. This effect of the trapped liquid tends to decrease with increasing TLF. It is also clear that the REE content of calculated liquids from bulk cumulates will be overestimated if the TLF is not taken into account. Moreover, an independent estimate of the TLF should be available (e.g., through the P_2O_5 content) because, as revealed by the high variability of the TLF in pimo-C cumulates of BKSK, a single evaluation of the TLF in different cumulates for the application of the EDM might be incorrect.

7. The closed-system crystallization of trapped liquid

Many authors have considered the problem as to whether the intercumulus liquid crystallizes in situ as a closed-system or migrates through the crystal pile to eventually return to the overlying resident magma volume. Several mechanisms are believed to be responsible for melt migration. Studies of compositional convection (e.g., Tait et al., 1984; Tait and Jaupart, 1992) and compaction of partially molten rocks (e.g., McKenzie, 1984; Mathez et al., 1997; Meurer and Boudreau, 1998) have presented arguments for the redistribution of intercumulus liquid within and outside the mineral matrix at various stages of the compositional evolution of this melt. On the other hand, many workers have used incompatible element abundances as an indicator of the trapped melt fraction (e.g., Henderson, 1968; Campbell, 1977; Chalokwu and Grant, 1987; Cawthorn and Walsh, 1988; Wilson, 1992; Cawthorn, 1996). The concept of "trapped liquid shift," proposed by Barnes (1986), is also based on the assumption that the intercumulus liquid crystallized in a closed-system.

In this work, calculated liquids based on the composition of bulk cumulates have resulted in consistent results for REE, which certainly represent some of the most incompatible elements. This is a strong argument against significant migration of intercumulus melt, in accordance with other studies (e.g., Cawthorn et al., 1992). The adjective "trapped" can thus be applied to intercumulus liquid in BKSK.

8. Conclusions

REE concentrations in bulk cumulates from the Bjerkreim–Sokndal layered intrusion can be used to trace the relative influence of cumulus minerals and of trapped liquid on REE distribution. In leuconoritic cumulates, which do not have cumulus apatite, REE are controlled by the trapped liquid fraction and by the compositions and proportions of cumulus minerals. REE spectra for these cumulates are very similar to those of plagioclase, but the absolute REE content, as well as La/Sm, Eu/Eu* and $(La/Yb)_N$, are increasingly modified with the increasing proportion of trapped liquid. Assessment of the trapped liquid fraction in leuconorites reveals a variation from 2 to 25%. Reason for this wide range of TLF is probably different cooling rates in different parts of the intrusion depending on the distance to the gneissic margins. Cumulus apatite in gabbronorites buffers the REE distribution and imposes its spectra on the composition of bulk cumulates. The influence of the trapped liquid cannot be sorted out in gabbronorites due to the control by the modal proportion and composition of apatite.

Mass balance calculations based on bulk cumulate composition and on the modal proportions of cumulus minerals yield the REE composition of liquids in equilibrium with the most primitive troctolitic cumulates in BKSK. These REE distributions are similar to the parental magma of the intrusion for TLF values ranging from 20 to less than 5%, agreeing with estimates based on the P_2O_5 content. The reliability of liquid compositions for REE obtained from bulk cumulates argues against the migration of interstitial liquid, and favours closed-system crystallization.

Acknowledgements

This work was funded by the Belgian Fund for Joint Research and the Fund for Research in Industry and Agriculture (FRIA). Fieldwork was partly supported by the Paul Fourmarier Foundation.

Titania A/S is gratefully acknowledged for its support. This paper has benefited of constructive reviews from J. Bédard and J.R. Wilson.

References

Barnes, S.J., 1986. The effect of trapped liquid crystallization on cumulus mineral compositions in layered intrusions. Contributions to Mineralogy and Petrology 93, 524–531.

Barling, J., Weis, D., Demaiffe, D., 2000. A Sr-, Nd- and Pb-isotopic investigation of the transition between two megacyclic units of the Bjerkreim–Sokndal layered intrusion, south Norway. Chemical Geology 165, 47–65.

Bédard, J.H., 1994. A procedure for calculating the equilibrium distribution of trace elements among the minerals of cumulate rocks, and the concentration of trace elements in the coexisting liquids. Chemical Geology 118, 143–153.

Bédard, J.H., 2001. Parental magmas of the Nain plutonic suite anorthosites and mafic cumulates: a trace element modelling approach. Contributions to Mineralogy and Petrology 141, 747–771.

Bolle, O., Diot, H., Duchesne, J.C., 2000. Magnetic fabric and deformation in charnockitic igneous rocks of the Bjerkreim–Sokndal layered intrusion (Rogaland, Southwest Norway). Journal of Structural Geology 22, 647–667.

Bolle, O., Trindade, R.I.F., Bouchez, J.L., Duchesne, J.C., 2002. Imaging downward granitic magma transport in the Rogaland Igneous Complex, SW Norway. Terra Nova 14, 87–92.

Bolle, O., Demaiffe, D., Duchesne, J.C., 2003. Petrogenesis of jotunitic and acidic members of an AMC suite (Rogaland anorthosite province, SW Norway): a Sr and Nd isotopic assessment. Precambrian Research 124, 185–214.

Campbell, I.H., 1977. A study of macro-rhythmic layering and cumulate processes in the Jimberlana intrusion, Western Australia: Part 1. The upper layered series. Journal of Petrology 18, 183–215.

Cawthorn, R.G., 1996. Models for incompatible trace-element abundances in cumulus minerals and their application to plagioclase and pyroxenes in the Bushveld Complex. Contributions to Mineralogy and Petrology 123, 109–115.

Cawthorn, R.G., Walsh, K.L., 1988. The use of phosphorous contents in yielding estimates of the proportion of trapped liquid in cumulates of the upper zone of the Bushveld Complex. Mineralogical Magazine 52, 81–89.

Cawthorn, R.G., Meyer, P.S., Kruger, F.J., 1991. Major addition of magma at the Pyroxenite Marker in the western Bushveld Complex, South Africa. Journal of Petrology 32, 739–763.

Cawthorn, R.G., Sander, B.K., Jones, I.M., 1992. Evidence for the trapped liquid shift effect in the Mount Ayliff Intrusion, South Africa. Contributions to Mineralogy and Petrology 111, 194–202.

Chalokwu, C.I., Grant, N.K., 1987. Reequilibration of olivine with trapped liquid in the Duluth complex, Minnesota. Geology 15, 71–74.

Demaiffe, D., Hertogen, J., 1981. Rare earth element geochemistry and strontium isotopic composition of a massif-type anorthositic–charnockitic body: the Hidra massif (Rogaland, SW Norway). Geochimica et Cosmochimica Acta 45, 1545–1561.

Duchesne, J.C., 1972. Iron-titanium oxide minerals in the Bjerkrem–Sogndal Massif, South-western Norway. Journal of Petrology 13, 57–81.

Duchesne, J.C., 1978. Quantitative modeling of Sr, Ca, Rb, and K in the Bjerkrem–Sogndal layered lopolith (S.W. Norway). Contributions to Mineralogy and Petrology 66, 175–184.

Duchesne, J.C., 1987. The Bjerkreim–Sokndal massif. In: Maijer, C., Padget, P. (Eds.), The Geology of the Southernmost Norway. Norske Geologiske Undersøkelse Special Publication, pp. 56–59.

Duchesne, J.C., 2001. The Rogaland Intrusive Massifs, an excursion guide. NGU report 2001.29. Geological Survey of Norway. 137 pp.

Duchesne, J.C., Charlier, B., 2005. Geochemistry of cumulates from the Bjerkreim–Sokndal layered intrusion (S. Norway): Part I. Constraints from major elements on the mechanism of cumulate formation and on the jotunite liquid line of descent. Lithos (this issue).

Duchesne, J.C., Demaiffe, D., 1978. Trace elements and anorthosite genesis. Earth and Planetary Science Letters 38, 249–272.

Duchesne, J.C., Hertogen, J., 1988. Le magma parental du lopolithe de Bjerkreim–Sokndal (Norvège méridionale). Comptes Rendus de l'Académie des Sciences de Paris 306, 45–48.

Duchesne, J.C., Wilmart, E., 1997. Igneous charnockites and related rocks from the Bjerkreim–Sokndal layered intrusion (Southwest Norway): a jotunite (hypersthene monzodiorite)-derived A-type granitoid suite. Journal of Petrology 38, 337–369.

Duchesne, J.C., Roelandts, I., Demaiffe, D., Hertogen, J., Gijbels, R., De Winter, J., 1974. Rare-Earth data on monzonoritic rocks related to anorthosites and their bearing on the nature of the parental magma of the anorthositic series. Earth and Planetary Science Letters 24, 325–335.

Duchesne, J.C., Roelandts, I., Demaiffe, D., Weis, D., 1985. Petrogenesis of monzonoritic dykes in the Egersund–Ogna anorthosite (Rogaland, S.W. Norway): trace elements and isotopic (Sr, Pb) constraints. Contributions to Mineralogy and Petrology 90, 214–225.

Duchesne, J.C., Wilmart, E., Demaiffe, D., Hertogen, J., 1989. Monzonorites from Rogaland (Southwest Norway): a series of rocks coeval but not comagmatic with massif-type anorthosites. Precambrian Research 45, 111–128.

Dunn, T., Sen, C., 1994. Mineral/matrix partition coefficients for orthopyroxene, plagioclase, and olivine in basaltic to andesitic systems: a combined analytical and experimental study. Geochimica et Cosmochimica Acta 58, 717–733.

Henderson, P., 1968. The distribution of phosphorous in the early and middle stages of fractionation of some basic layered igneous rocks. Geochimica et Cosmochimica Acta 32, 897–911.

Hunter, R.H., 1996. Texture development in cumulate rocks. In: Cawthorn, R.G. (Ed.), Layered Intrusions. Elsevier, Amsterdam, pp. 77–101.

Irvine, T.N., 1980. Magmatic infiltration metasomatism, double-diffusive fractional crystallization, and adcumulus growth in the

Muskox intrusion and other layered intrusions. In: Hargraves, R.B. (Ed.), Physics of Magmatic Processes. Princeton University Press, Princeton, NJ, pp. 325–384.

Irvine, T.N., 1982. Terminology for layered intrusions. Journal of Petrology 23, 127–162.

Jensen, J.C., Nielsen, F.M., Duchesne, J.C., Demaiffe, D., Wilson, J.R., 1993. Magma influx and mixing in the Bjerkreim–Sokndal layered intrusion, South Norway: evidence from the boundary between two megacyclic units at Storeknuten. Lithos 29, 311–325.

Jensen, K.K., Wilson, J.R., Robins, B., Chiodoni, F., 2003. A sulphide-bearing orthopyroxenite layer in the Bjerkreim–Sokndal intrusion, Norway: implications for processes during magma-chamber replenishment. Lithos 67, 15–37.

Maier, W.D., Barnes, S.-J., 1998. Concentrations of rare earth elements in silicate rocks of the Lower, Critical and Main Zones of the Bushveld Complex. Chemical Geology 150, 85–103.

Mathez, E.A., Hunter, R.H., Kinzler, R., 1997. Petrologic evolution of partially molten cumulate: the Atok section of the Bushveld Complex. Contributions to Mineralogy and Petrology 129, 20–34.

McKenzie, D.P., 1984. The generation and compaction of partially molten rock. Journal of Petrology 25, 713–765.

Meurer, W.P., Boudreau, A.E., 1998. Compaction of igneous cumulates: Part I. Geochemical consequences for cumulates and liquid fractionation trends. Journal of Geology 106, 281–292.

Meurer, W.P., Klaber, S., Boudreau, A.E., 1997. Discordant bodies from olivine-bearing zones III and IV of the Stillwater Complex, Montana—evidence for postcumulus fluid migration and reaction in layered intrusions. Contributions to Mineralogy and Petrology 130, 81–92.

Michot, P., 1960. La géologie de la catazone: le problème des anorthosites, la palingenèse basique et la tectonique catazonale dans le Rogaland méridional (Norvège méridionale). Int. Geol. Congr., XXI Session, Guide to Excursion A, vol. 9, pp. 54.

Morse, S.A., 1979. Kiglapait geochemistry: II. Petrography. Journal of Petrology 20, 591–624.

Nielsen, F.M., Wilson, J.R., 1991. Crystallization processes in the Bjerkreim–Sokndal layered intrusion, south Norway: evidence from the boundary between two macrocyclic units. Contributions to Mineralogy and Petrology 107, 403–414.

Paludan, J., Hansen, U.B., Olesen, N.Ø., 1994. Structural evolution of the Precambrian Bjerkreim–Sokndal intrusion, South Norway. Norsk Geologisk Tidsskrift 74, 185–198.

Robins, B., Tumyr, O., Tysseland, M., Garman, L.D., 1997. The Bjerkreim–Sokndal layered intrusion, Rogaland, SW Norway: evidence from marginal rocks for a jotunite parent magma. Lithos 39, 121–133.

Roelandts, I., 1975. Contribution au dosage par activation neutronique des terres rares et d'autres elements en trace dans les roches magmatiques, PhD thesis, University of Liège, Unpublished.

Roelandts, I., Duchesne, J.C., 1979. Rare-earth elements in apatite from layered norites and iron-titanium oxide ore-bodies related to anorthosites (Rogaland, S.W. Norway). In: Ahrens, L.H. (Ed.), Origin and Distribution of the Elements. Pergamon Press, Oxford, pp. 199–212.

Sparks, R.S.J., Huppert, H.E., Kerr, R.C., McKenzie, D.P., Tait, S.R., 1985. Postcumulus processes in layered intrusions. Geological Magazine 122, 555–568.

Sun, S.-S., McDonough, W.F., 1989. Chemical and isotopic systematics of oceanic basalts: implication for mantle composition and process. In: Saunders, A.D., Norry, M.J. (Eds.), Magmatism in the Ocean Basins, Spec. Publ. Vol. Geol. Soc. Lond., pp. 313–345.

Tait, S., Jaupart, C., 1992. Compositional convection in a reactive crystalline mush and melt differentiation. Journal of Geophysical Research 97, 6735–6756.

Tait, S.R., Huppert, H.E., Sparks, R.S.J., 1984. The role of compositional convection in the formation of adcumulus rocks. Lithos 17, 139–146.

Vander Auwera, J., Longhi, J., 1994. Experimental study of a jotunite (hypersthene monzodiorite): constraints on the parent magma composition and crystallization conditions (P, T, fO2) of the Bjerkreim–Sokndal layered intrusion (Norway). Contributions to Mineralogy and Petrology 118, 60–78.

Vander Auwera, J., Bologne, G., Roelandts, I., Duchesne, J.C., 1998a. Inductively coupled plasma-mass spectrometric (ICP-MS) analysis of silicate rocks and minerals. Geologica Belgica 1, 49–53.

Vander Auwera, J., Longhi, J., Duchesne, J.C., 1998b. A liquid line of descent of the jotunite (hypersthene monzodiorite) suite. Journal of Petrology 39, 439–468.

Vander Auwera, J., Longhi, J., Duchesne, J.C., 2000. The effect of pressure on DSr (plag/melt) and DCr (opx/melt): implications for anorthosite petrogenesis. Earth and Planetary Science Letters 178, 303–314.

Watson, E.B., Green, T.H., 1981. Apatite/liquid partition coefficients for the rare earth elements and strontium. Earth and Planetary Science Letters 56, 405–421.

Wilmart, E., Demaiffe, D., Duchesne, J.C., 1989. Geochemical constraints on the genesis of the Tellnes ilmenite deposit, Southwest Norway. Economic Geology 84, 1047–1056.

Wilson, A.H., 1992. The geology of the Great Dyke, Zimbabwe: crystallization, layering, and cumulate formation in the P1 pyroxenite of cyclic unit 1 of the Darwendale subchamber. Journal of Petrology 33, 611–663.

Wilson, J.R., Robins, B., Nielsen, F.M., Duchesne, J.C., Vander Auwera, J., 1996. The Bjerkreim–Sokndal layered intrusion, Southwest Norway. In: Cawthorn, R.G. (Ed.), Layered Intrusions. Elsevier, Amsterdam, pp. 231–255.